Energy Science & Engineering

ORIGINAL ARTICLE OPEN ACCESS

A Comparative Study of *Litchi-chinensis* Biodiesel–Diesel Blends With Alcoholic and Nanoparticle Additives on Engine Performance, Emissions, and Coefficient of Friction

Tahir Asif[1] | Tehreem Rizwan[1] | Saad Jahangir[1] | Fahad Noor[2] | Adnan Qamar[2] | Muhammad Ali Shahbaz[1] | Muhammad Mujtaba Abbas[2] | Fahid Riaz[3]

[1]Automotive Engineering Centre, University of Engineering and Technology, Lahore, Pakistan | [2]Department of Mechanical Engineering, University of Engineering and Technology, New Campus, Lahore, Pakistan | [3]College of Engineering, Abu Dhabi University, Abu Dhabi, UAE

Correspondence: Muhammad Ali Shahbaz (alishahbaz@uet.edu.pk) | Fahid Riaz (fahid.riaz@adu.ac.ae)

Received: 4 February 2025 | **Revised:** 30 June 2025 | **Accepted:** 1 July 2025

Funding: The authors acknowledge Abu Dhabi University for partially funding this research.

Keywords: cold flow characteristics | engine performance | litchi biodiesel | nanoparticle additives | sustainable fuels

ABSTRACT

Environmental hazards and the growing demand for fossil fuels are two major current concerns. The current global situation requires extensive research on renewable fuels. In this experimental study, we investigated different blends of biodiesel derived from litchi seed oil, which is inedible, for engine performance, emissions, and tribological characteristics. *Litchi chinensis* biodiesel was synthesized from litchi seed oil through a microwave-assisted transesterification. First, a 30% biodiesel–diesel blend (B30) was prepared and mixed with ethyl ethanoate (EE) in the proportions of 10% (B30EE10) and 15% (B30EE15) by volume. Additionally, 100 ppm of aluminum oxide (abbreviated as Al) nanoparticles were added in all blends (B30Al, B30EE10Al, and B30EE15Al). All six blends were investigated for engine performance and emissions on a diesel engine. The coefficient of friction (COF) was measured using a four-ball tribo-tester for a 5% by volume fuel blend in SAE-40 lubricant (ASTM D4172 standard). Engine performance analyses indicated that, compared to diesel, the B30EE10Al gives most promising results at an engine speed of 1500 min^{-1} in terms of engine performance and emissions with 4.97% higher brake thermal efficiency and by reducing brake-specific fuel consumption, and CO, HC, and NO_x up to 15.27%, 30.24%, and 3.92%, respectively. Four-ball tribo-tester results reveal that 5% B30Al in SAE-40 oil has the lowest COF of 0.066, which is 34% less than that of diesel. Overall, the addition of aluminum nanoparticles and EE10 in *Litchi chinensis* biodiesel blend has improved the fuel quality in terms of performance and emission properties.

1 | Introduction

The increasing fossil fuel consumption to meet the energy requirements of transportation vehicles, which are heavily dependent on petrol and diesel engines, is a major global issue [1]. Diesel engines, being more energy-efficient and cost-effective, are utilized more often compared to their petrol counterparts [2]. Because of the rapidly depleting fossil fuels and the severe consequences of greenhouse gases (GHGs), researchers are looking for innovative energy solutions and fuel sources that can be helpful in the face of this global challenge [3, 4].

Biodiesel is an excellent alternative fuel for diesel engines because of its superior physicochemical properties [5]. This concept has led to the use of many novel resources for biodiesel production, like *Prosopis juliflora* [6], *Pontederia crassipes*, and *Trichosanthes cucumerina* [7], etc. However, the controversy over fuel versus food and the expensive cost of feedstock for biodiesel synthesis make the nonedible or waste material feedstock more desirable as an alternative energy resource [8]. A recent review found that nonedible oils can be used as a biodiesel feedstock, improve storability, engine performance, and physical attributes of diesel blends [9].

Numerous researchers have looked at various renewable biofuels, such as alcohols, vegetable oils, and biodiesel [10–13]. In this proposed study, *Litchi chinensis* seed biodiesel is being used to prepare a fuel blend with 30% biodiesel in 70% diesel by volume (B30). The litchi seed contains methylene cyclopropylalanine, which is toxic in nature and thus cannot be used as a food source [14]. The oil extracted from the starch of litchi seeds can be processed and utilized as biofuel, which not only reduces the environmental damage due to tailpipe emissions but is also workable for organic waste management [15, 16]. Fatty acid compositions have a significant impact on the cold flow characteristics and oxidation stability of biodiesel [17]. Properties of litchi biodiesel reveal high unsaturated fatty acids and good cold flow characteristics [18].

The commercialization of biodiesel has met many compositional and functional obstacles despite its superior physicochemical qualities [5, 19, 20]. The commercial feasibility of biofuels is also challenged due to poor cold flow characteristics [21]. The method of biodiesel production also affects the quality of fuel. A comparison of soybean biodiesel production reveals that fuel obtained from transesterification has produced better results in terms of engine performance and emission characteristics than that of the pyrolysis method [22]. However, some fuels have been found to have better properties than others. Castor oil has a workable cloud point and viscosity because it contains fatty acid ethyl ester (FAEE) [23]. Because of lower pour and cloud point values, castor-based biodiesel performs well in cold areas and has good lubricity [24]. Litchi biodiesel is expected to have better cold flow properties due to its high unsaturated fatty acids [18].

By using innovative techniques, such as adding oxygenated alcohols and nanoparticle additives, these disadvantages can be overcome and potentially improve the performance of diesel engines running on biofuels [25, 26]. The use of additive nanoparticles and oxygenated additives (mainly alcohols) can complement both the good and poor qualities of biodiesel. Table 1 summarizes the notable discoveries from similar studies on the effects of biodiesel–diesel blends, nanoparticles, and alcoholic additives on diesel engines.

Fuel mix properties may differ in combination with other fuels; a 20% palm biodiesel–diesel blend mixed with *n*-butanol and diethyl ether gives higher brake thermal efficiency (BTE) than the same additive concentrations in jatropha biofuel. Similarly, ethanol demonstrated a visible reduction in emission compared to *n*-butanol and diethyl ether [35]. Combustion of palm biodiesel with diesel shows a drop in brake-specific fuel consumption (BSFC), which further reduces with oxyhydrogen (HHO) gas inclusion, indicating that the addition of both oxygen and hydrogen improves the combustion efficiency of fuel blends [36]. Ten percent by volume of dimethyl carbonate (DMC) in a 40% sapota seed biodiesel–diesel blend resulted in lower smoke, hydrocarbon (HC), and carbon monoxide (CO) emissions when studied under 10% exhaust gas recirculation (EGR) [37]. Di-tetra-butyl-peroxide (DTBP) improves the BTE of a 50%–50% papaya seed biodiesel–diesel blend with reduced smoke, CO, and HC in exhaust gases, particularly owing to its high oxygen content [38].

The alcohols have high latent heat of evaporation; thus, their addition to the fuel blends reduces the NO_x formation [39]. In comparison, the oxygenated additives are more effective in soot reduction than esters (biodiesels) having the same mass fraction of oxygen [39–41]. Higher level alcohols show more overall improvement in engine combustion, performance, and emission characteristics compared to lower alcohols (butanol) in a mix of 30% oleander methyl ester and carbon nanotubes (CNTs) [42].

Ahmad et al. [43] worked on oxygenated additives in second-generation biodiesels and concluded that the BSFC mostly increased with the inclusion of oxygenated agents. In another study, 12% diethyl ether in a 20% tamarind-seed biodiesel–diesel blend gives a significant drop in harmful emissions [44]. Similarly, 5%–15% 2-ethoxy ethyl acetate blends in diesel enhanced engine performance and implicitly lowered the tailpipe emissions [45].

Ethyl ethanoate (EE) was used in this study as an oxygenated additive. In literature, 5%–10% of EE showed a considerable drop in emissions along with a minimal rise in fuel consumption of biodiesel–diesel blend [29]. EE is a renewable fuel additive, and its high oxygen level gives the NO_x-PM trade-off as well as NO_x-BSFC trade-off properties without any thermal efficiency losses in a diesel engine [29, 46]. Aguado-Deblas et al. [47] studied the effects of EE in sunflower and castor oil biofuel blends and observed higher fuel consumption due to lower calorific value (CV), reduction of soot owing to low cetane number, better combustion at low temperatures, and lower emission. Different proportions (5.65%, 10.65%, and 15%) of EE in neat diesel give lower values of heat release rate and in-cylinder peak pressure and increased CO and HC. At 15% EE, engine performance was stable with less NO_x emission and 15.35% less BSFC [30]. It is also observed, from the previous studies, that the use of EE as an additive in biofuels, up to 15% by volume, does not cause any issues related to engine operation. Furthermore, its good miscibility makes it desirable to use in biodiesel–diesel blends and improves the quality of the fuel mix [29]. EE also shows better cold flow properties when added with castor oil and waste cooking oil [47].

Despite significant NO_x reduction qualities and high oxygen content of oxygenated additives, their low cetane number and poor lubricating qualities make them difficult to employ as a fuel enhancer in diesel engines [5, 48]. On the other hand, nanoparticles show superior results in terms of brake power (BP), BSFC, and BTE of the engine and in lowering NO_x and HC [28]. Researchers have been testing the effectiveness of using biodiesel–diesel blends in place of neat diesel by employing a variety of additives in different combinations to enhance the physiochemical properties of these renewable fuels [49].

TABLE 1 | Key findings from several studies involving the use of biodiesel–diesel blends, nanoparticles, and alcoholic additives in diesel engines and analysis of their performance, emission, and tribological characteristics. Upward arrows show an increase, and downward arrows represent a decrease.

Author	Sample blends	Findings		
		Performance parameters	Emission characteristics	Coefficient of friction
Mujtaba et al. [27]	B10 (diesel) B30 B30CNT $B30TiO_2$ B30DMC B30DEE	BSFC↑↓ BTE↑	HC↓ (except for B30 + CNT) CO↓ NO_x↑ (except for B30 + CNT)	—
Ağbulut et al. [28]	D100 (diesel) B10 (90% diesel–10% of waste cooking oil biodiesel) $B10TiO_2$ (B10 with 100 ppm of titanium oxide) $B10Al_2O_3$ (B10 with 100 ppm of aluminum oxide) $B10SiO_2$ (B10 with 100 ppm of silicon oxide)	BSFC↓ (except for B20) BTE↑ (except for B20)	CO↓ NO_x↓ HC↓	—
Çakmak [29]	D80B20 (0% ethyl ethanoate, 20% of an EN 14214 standard biodiesel, and 80% diesel) D80B15EE5 D80B10EE10	—	CO↓ NO_x↓	—
Musyoka et al. [30]	D100 (100% diesel, 0% *n*-butanol, and 0% ethyl ethanoate) Bu10.65 D85Bu15 D80Bu20 D94.35EE5.65 D89.35EE10.65 D85EE15	BSFC↓↑	NO_x↓ CO↑ HC↑	—
Soudagar et al. [31]	D80HOME20 (20% honge oil methyl biodiesel, 80% diesel, and 0ppm Al_2O_3) D80HOME20Al20 D80HOME20Al40 D80HOME20Al60	BTE↓ BSFC↑	HC↑ NO_x↑ CO↑	—
Fayad and Dhahad [32]	Diesel B20 (0 mg/L Al_2O_3, 20% butanol, and 80% diesel) B20Al30 B20Al50 B20Al100	BSFC↓ (except for B20) BTE ↑	NO_x↓ (except for B20, i.e., NO_x↓↑) CO↓ HC↓ CO_2↑	—
Mujtaba et al. [33]	B10 (diesel) B30	BSFC↓↑ BTE↑	HC↓ CO↓	COF↓

(Continues)

TABLE 1 | (Continued)

Author	Sample blends	Findings: Performance parameters	Findings: Emission characteristics	Findings: Coefficient of friction
	$B30TiO_2$		NO_x↑	
	B30DMC			
	Tribological samples: 5% of each fuel blend in 95% SAE 40 base lubricant			
Mujtaba et al. [34]	SAE 40 lubricant	—	—	COF↓
	5% B10 (diesel) + lubricant			
	5% B30 (30% palm–sesame [50–50] biodiesel) + lubricant			
	5% (B30DMC20) + lubricant			
	5% (B30Eth10) + lubricant			
	5% (B30CNT100) + lubricant			
	5% ($B30TiO_2100$) + lubricant			

Nanoparticle additives, usually metal-based oxides or carbon-containing compounds, are also desirable in fuel quality improvement in biodiesel [26]. Previous research has shown that carbon-based nanoparticles like CNTs and GO (graphene oxide), as well as metallic nanoparticles like CuO, ZnO, MnO, TiO_2, CeO_2, Al_2O_3, and Fe_2O_3, have shown remarkable outcomes. By achieving high BTE and high BP and lowering carbon emissions and NO_x, the mentioned nanoparticle additives seem to improve engine performance [26, 50–52].

Metal-oxide-based nanoparticle additives enhance the heating value of biodiesel and improve viscosity and cetane number. A 10% waste cooking oil biodiesel blend (B10), evaluated against the inclusion of 100 ppm nanoparticles of Al_2O_3, TiO_2, and SiO_2 in B10 biofuel, the maximum decrease in CO was observed with Al_2O_3 addition due to its higher oxygen content [28]. Al_2O_3 also improved the combustion process by enhancing in-cylinder pressure and heat release rate when studied in Juliflora oil biodiesel [53]. Two different biofuel blends, 20% honge oil biodiesel–diesel with aluminum and 20% dairy scum biodiesel–diesel blend mixed with graphene oxide nanoparticles, were investigated by Soudagar et al. [31, 54]. Their findings revealed that 40 ppm of both aluminum and graphene nanoparticles in two biodiesels reduced CO by 48.43% and 38.66%, respectively; 50 ppm of Al_2O_3 in 20% mahua biofuel enhances the fuel atomization and thermal efficiency and reduces the emissions by 15%–30% for NO_x, HC, smoke, and CO [55, 56].

The addition of 100 ppm Al_2O_3 to a 20% butanol blend in 80% neat diesel (B20 butanol–diesel blend) improves emissions and combustion [32]. Al_2O_3 and CeO_2, 100 ppm of each when analyzed in a B20 mixture of mahua biodiesel give similar results with 100 ppm of Al_2O_3 in a B20 butanol–diesel blend [32, 57]. On the other hand, graphical results of Al_2O_3 and CeO_2, 150 ppm each in a B20 mixture of mahua biodiesel, show increased NO_x, specifically at higher loads, and an irregular trend of CO and HC emissions with increasing load, potentially caused by combustion instability [57]. Aalam et al. [58] performed an experimental study using a 25% Ziziphus jujube methyl ester (ZJME25) blend and got similar results as in Hameed and Muralidharan's work [57]. The addition of Al_2O_3 gives further rise to the NO_x emission in the ZJME25 blend. To sum it all up, the use of different fuel additives along with biodiesel blends is becoming popular in the engine research fraternity [59, 60].

Tribological properties of fuel are also important for the long-lasting operation of engines. The tribological studies are mainly concerned with minimizing coefficient of friction (COF) between mechanical surfaces [61]. Lubricant oils are used to improve tribological properties and are continuously worked on to explore enhanced characteristics to minimize wear by the inclusion of solid nanoparticles and liquid additives. Nanoparticles reduce the degradation of lubricating oil by forming a layer between metallic surfaces [34]. Study of the tribological aspects of biodiesel fuel is vital, as fuel blends can penetrate through the ring–piston–cylinder assembly and thus affect the lubricity of engines by polluting the engine lubricating oil. Literature shows that it can make up to 5% of total lubricant volume [33, 62].

According to Kumar et al. [63], castor biodiesel has better physicochemical characteristics and reduced COF when compared to synthetic 20W-40 base oil. In a study related to novel *Jasminum officinale* biodiesel blends, the lubricity of the tested fuels rises with the addition of biodiesel concentration at all the tested conditions [64]. Other studies have shown improved tribological behavior of the biofuels with MgO, graphene, and Al_2O_3 nanoparticles [65]; 1 wt.% graphene nanoparticles in neem oil, when tested under ASTM standards and four-ball tribo-tester, a reduced COF with smoother wear scar diameter (WSD) was observed [66]. A study by Ghalme et al. [67] shows that the optimal value of 0.5 wt.% of Al_2O_3 nanoparticles improved WSD and COF at all loading conditions. Independent of its concentrations in biodiesel–diesel blends, Al_2O_3 had the highest antiwear performance among the nanofuels studied in filtered tire pyrolysis oil biodiesel [68]. Overall, Al_2O_3 nanoadditives reveal the best traits even in terms of price, load, speed, and low concentration usage [65]. The performance improvement is due to the self-protective film formed by Al_2O_3 nanoparticles on the frictional surfaces, which occurs in response to its ball bearing effect [67]. Mujtaba et al. [33, 34] used a four-ball tribo-tester to evaluate COF and WSD of SAE-40 and mineral lubricating oils with a 30% palm–sesame biodiesel (50% palm oil, 50% sesame oil) blend with 70% diesel and 100 ppm TiO_2 or 20% DMC as additives and found improved lubricity with TiO_2 blended fuel and less COF, less WSD, and good engine and emission performance of DMC diluted 30% 50P50S–diesel fuel.

In this study, a 30:70 ratio of *Litchi-chinensis* biodiesel and diesel was used to prepare the biodiesel–diesel blend (B30). To improve the fuel characteristics, such as cold start performance, engine wear, and emissions, a novel approach of investigating safe concentrations, 10%–15% by volume of an economical oxygenated additive, EE, and 100 ppm aluminum oxide (Al_2O_3, abbreviated as Al in the following text) nanoparticles combined with 30% *Litchi-chinensis* biodiesel–diesel blend was used. The main objectives of this work were to develop innovative blends of litchi biodiesel with EE and Al as fuel additives and examine these blends for improvements in the engine's performance and emission characteristics and tribological properties. These tests provide practical insights into optimizing these blends for real-world applications.

1.1 | The Novelty of the Present Work

Biodiesel derived from various feedstocks, additives to enhance their properties, and results from engine testing are discussed in Section 1. However, studies specifically addressing *Litchi-chinensis* seed oil (LSO) biodiesel are only limited to oil extraction and properties. This research aims to cover the gap by experimentally testing *Litchi-chinensis* biodiesel produced from fast and efficient microwave-assisted transesterification with a waste-derived catalyst for promoting sustainable and clean energy in alignment with UN SDGs 7 and 13.

The combination of binary (LSO biodiesel–diesel) and ternary (LSO biodiesel–diesel–EE) blends mixed with Al nanoparticles in the specific compositions used in this study has not been explored in past works. The study is focused on determining engine performance, combustion, and emission characteristics. In addition to this, experimental investigation also includes tribological aspects of various blends.

2 | Materials and Methods

2.1 | Biodiesel: Production and Recovery

The microwave-assisted transesterification process was used to produce biodiesel from LSO. Time, stirrer speed, methanol concentration, and catalyst concentration all impact the biofuel production from this process. The catalyst was extracted by calcination of 2 kg of dry potato waste, and the potassium hydroxide (KOH) catalyst was recovered from the ash solution. To maintain the temperature at 64°C, the microwave oven was run at 30% power. Glycerin separation occurred when the solution was stored for 8 h. After that, the biodiesel was heated to 100°C for 30 min to remove any remaining water content and later washed with hot distilled water. The properties of the LSO biodiesel product are presented in Table 2. A brief pictorial representation of the process is displayed in Figure 1. Further details on the experimental parameters and equipment details can be found in our previous work, focusing on the biodiesel production [18].

2.2 | Preparation of Fuel Blends

In addition to commercial diesel, six blends were prepared in this work. The fuel blend compositions are given in Table 3 along with the nomenclature to be used throughout the study. For fuel blend compositions, the basic biodiesel–diesel blend was formed in 30–70 proportions, thus called B30 throughout the following text. The primary sample size taken for the B30 blend is 1000 and 100 g for each engine and tribological testing cycle, respectively. Initially, diesel and biodiesel prepared with transesterification were mixed in a container, and the solution was stirred well. Without using heat, the mixture was agitated for 10 min. After a uniform B30 blend was formed, the alcoholic additive EE and the Al nanoparticles (20–30 nm, spherical shape) [73] were added in the decided proportions. The prepared fuel blends were then simultaneously heated and subjected to mechanical stirring using a hot plate magnetic stirrer (Heidolph MR Hei-End) for 10 min at 1000 revolutions per minute (rpm) and at a temperature of 60°C to achieve an initial uniform distribution of nanoparticles. This step ensures that larger agglomerates are broken down and dispersed throughout the blend to get homogenized ternary blends (diesel + biodiesel + EE) [26].

Following mechanical stirring, the blends were treated using an ultrasonic bath (Elma E100H), operating at 37 kHz for 60 min. Sonication [74] was done to ensure the dispersion of aluminum oxide nanoparticles in B30 and B30 + EE blends. This technique agitated the solution with sound waves, which aided in the formation of a uniform dispersion of the mixed solution. Ultrasonication is widely recognized for its ability to deagglomerate nanoparticles and achieve a stable colloidal suspension by generating cavitation forces that further break down any

TABLE 2 | The properties of LSO biodiesel compared to international standards.

Properties	Units	WCO biodiesel [69]	Diesel [70]	LSO B100 [18]	ASTM D6751 [71]	EN14214 [72]
Oxidative stability	h	4.61	13.20	6.1	3	6
Cetane no.		61	48.50	53.2	> 47	> 51
Calorific value	MJ/kg	38.76	46.6	38.8	—	—
Acid value	mg KOH/g	0.13	0.15	0.25	< 0.50	0.50
Viscosity at 40°C	mm^2/s	5.01	2.91	4.4	1.9–6	3.5–5
Density at 15°C	kg/m^3	862.1	842	875	870–900	860–900
Flashpoint	°C	154	78.50	175	> 130	> 120
Pour point	°C	12	2	0.3	−15 to 16	—
Cloud point	°C	2	2	6.59	−3 to 12	—
Cold filter plugging point	°C	7	0	−2.34	19 (max)	—

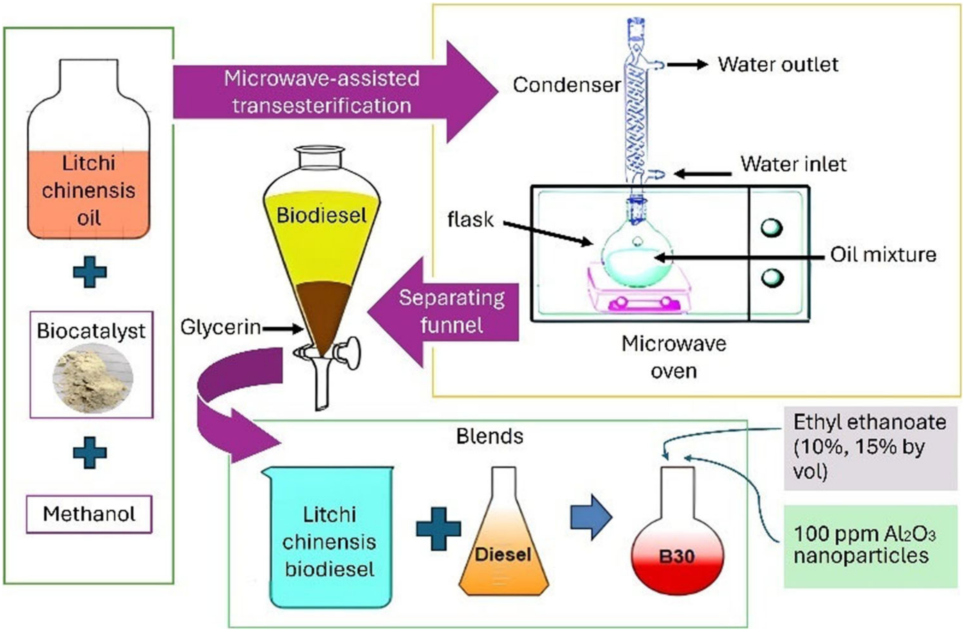

FIGURE 1 | Schematic display of biodiesel development and blend formation process. The litchi seed oil presented on the left went through esterification to transform into biodiesel. That was then mixed with diesel to form B30 and further blends (concentrations are mentioned in Table 3).

TABLE 3 | Fuel blend compositions of diesel, *Litchi chinensis* biodiesel, oxygenated additive EE, and Al nanoparticles.

Fuel blends	Biodiesel–diesel % composition	EE/percentage volume to B30 blend	Al/concentration parts per million (ppm)	Nomenclature
1	0–100	0	0	B0 (diesel)
2	30–70	0	0	B30
3	30–70	10	0	B30EE10
4	30–70	15	0	B30EE15
5	30–70	0	100	B30Al
6	30–70	10	100	B30EE10Al
7	30–70	15	100	B30EE15Al

TABLE 4 | Properties of fuel blends.

Properties	B0 (diesel)	B30	B30EE10	B30EE15	B30Al	B30EE10Al	B30EE15Al
Density at 15°C	842	851	848.2	850.5	854	855	856
Viscosity at 40°C	2.91	3.471	2.451	2.105	3.601	2.721	2.331
Calorific value	46.6	40.671	39.162	38.352	38.562	38.236	37.841

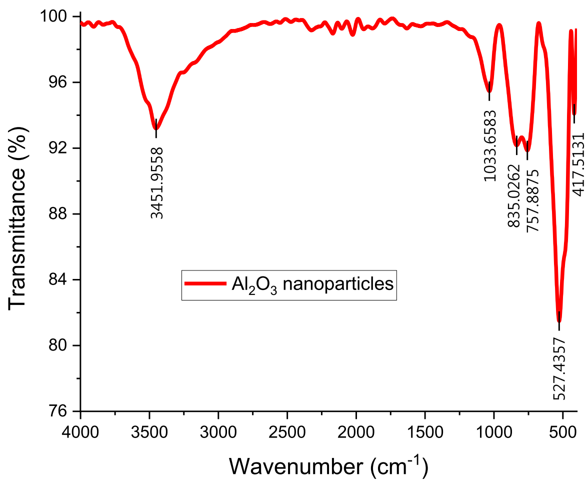

FIGURE 2 | FTIR spectrum of Al nanoparticles.

TABLE 5 | Engine specifications.

Factors	Values
Cylinders	03
Stroke	04
Compression ratio	16.5
Displacement	2.5 L
Max. power	50 Hp @2250 rpm
Max. torque	172 N m @1400 rpm
Static injection timing	16 degree BTDC
Nozzle opening/injection pressure	190 bar
Lubricant capacity	6/17 L
Cooling	Water type

remaining clusters of Al nanoparticles. Al nanoparticles are used in 100 ppm, while EE is added in 10% and 15% by volume. The blends were investigated for the dispersion stability of the Al nanoparticles, and no significant agglomeration or sedimentation was noticed over 7 days. This ensures that the nanoparticles are highly stable within the host fluid. This increased stability of the nanoparticles accounts for the series of schemes followed, that is, magnetic stirrings followed by ultrasonication, which broke down the nanoparticle aggregates within the host fluid and made their uniform dispersion possible. Also, the nanoparticles are spherical in shape and more stable in high-viscosity fluids compared to low-viscosity fluids [75]. This is another parameter that ensures their long-term stability. The presence of EE in the fuel blend may further enhance dispersion stability due to its polarity and solvent properties, which help reduce nanoparticle aggregation by modifying the surface tension and improving compatibility between the fuel components and nanoparticles [76]. Given that the prepared fuel blends were used within 48 h of preparation for all engine and tribological testing, the observed stability during this time frame ensured reliable and repeatable results.

Before engine test performance, a few properties including CV, density, and viscosity, were determined for fuel blend samples to observe the effects of additives. These properties are exhibited in Table 4.

2.3 | Characterization of Nanoparticles

Al nanoparticles used in this study are sourced from Nanostructured & Amorphous Materials Inc., USA, and have an average particle size of 20–30 nm and spherical morphology. The FTIR spectrum of sample nanoparticles is shown in Figure 2, which gives significant information about the bond structure and composition of nanoparticles under study. The spectroscopy was performed for the 4000–400 cm^{-1} wavelength range. The noteworthy infrared transmittance peaks can be observed at 3451.96, 1033.66, 832.133, 757.888, 527.436, and 417.513 cm^{-1}. The first peak at 1033.66 cm^{-1} with a transmittance of 95.46% indicates the presence of a hydroxyl group at the surface due to moisture. A characteristic peak at 1033.66 cm^{-1} confirms it to be an oxide. At 832.133 and 757.888 cm^{-1}, two fingerprint peaks are attributed to metal-oxide bond vibration in Al_2O_3. The sharp peak at 527.436 cm^{-1} and distinctive peak at 417.513 cm^{-1} are due to lattice vibrations of the Al–O–Al bond, which is a signature characteristic of Al_2O_3.

2.4 | Experimental Setup: Engine and Emission Analyzer

The experimental setup consists of a diesel engine (Perkins/AD 3.152) test bench loaded with a series of water heaters. The auxiliaries include a fuel tank, control panel, startup battery, an emission monitoring system (EMS) analyzer, and a display board with various load breakers. The water heaters act as a load on the system by receiving its voltage and current from the engine on the test bench. Specifications of the engine used for the experimentation are displayed in Table 5.

Figure 3 shows a model picture, and Figure 4 is a schematic representation of the test engine configuration. Engine testing was done by increasing engine speed at intervals of 100 rpm from 1000 to 1500 rpm while maintaining a constant load of 4500 W. To keep the engine running on the required load conditions, a total of nine heaters were powered from the test engine setup, each consuming 500 W of energy.

An auxiliary fuel tank was used to get the rate of fuel consumption for each test sample of 100 mL. At the same time, the voltage and current data from the display panel were recorded. The performance was then assessed at each of the engine speeds for the fuel blend combinations as indicated in Table 3. BSFC, BTE, and BP were calculated for performance assessment. At each engine speed, the exhaust values of HC, CO, and NO_x were measured from the EMS analyzer. The specifications of the EMS are mentioned in Table 6.

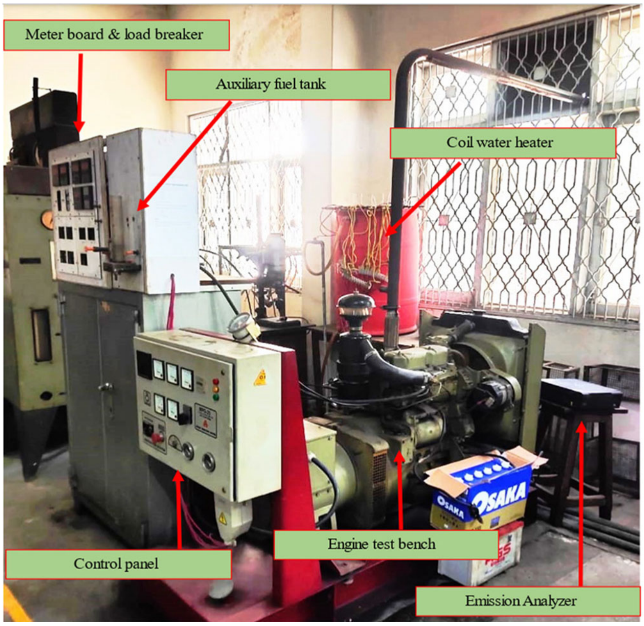

FIGURE 3 | The basic arrangement and components of the diesel engine test bench.

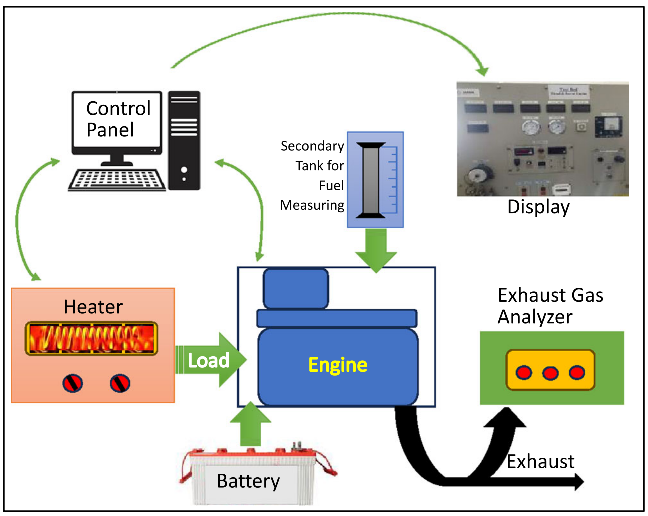

FIGURE 4 | A schematic representation of all the main and auxiliary parts of the engine setup (dimensions not to scale).

2.5 | Four-Ball Tribo-Testing

The COF in engine functions is affected by a number of variables, including lubricant type, environmental temperature, load, speed, and additives that may enter the lube oil during engine operation. By tracking the COF over time and observing its variation during the experimentations, one may gain insight into the lubricant's performance in dynamic situations. This information is useful for determining the behavior of lubricant across a range of time intervals and may also be used to evaluate how well it reduces wear and friction over longer working times. To get that information, a four-ball tribo-tester was used in the current study. The COF was determined at various test phases by tracking the frictional torque over time, and data on the COF throughout those time periods were obtained from it. The frictional forces between the surfaces of the revolving steel ball and the stationary balls coated with lubricant, as presented schematically in Figure 5, were monitored intermittently during the test.

The effect of 5% of all seven fuel blends on the COF of SAE-40 base lubricant was investigated using an automatic four-ball tribo-tester (MMW-1, Computer Servo Control Vertical Universal Friction and Wear Testing Machine). Four carbon–chromium steel balls were submerged in the mix of 95% SAE-40 standard lubricant oil and 5% sample fuel blends. Three fixed steel balls were attached to a temperature sensor and placed in a cup holder. The fourth ball was adjusted on the top rotating shaft. The temperature of the setup was kept constant when the speed of the rotating shaft was 1200 rpm A new set of four carbon–chromium steel balls was used for each repeated cycle of the experimentation as all seven of the fuel–lubricant mixtures were tested under the ASTM D4172 standard. The four-ball tribo-tester's operating parameters under given conditions are presented in Table 7.

2.6 | Calculations: BSFC, BTE, and COF

Fuel blends were tested for the quantity of 100 mL samples for each measurement. The rate of fuel consumed ($\dot{m}$) was noted

TABLE 6 | Specifications of EMS gas analyzer.

	Technique used	Emission type	Measurement range	Resolution
EMS analyzer	NDIR analyzer (nondispersive infrared)	CO	0%–10% vol.	± 0.001% vol.
	CLD-type (chemiluminescence detector) heated vacuum	NO_x	0–5000 ppm	± 1 ppm
	FID (flame ionization detector)	HC	0–9999 ppm	± 1 ppm

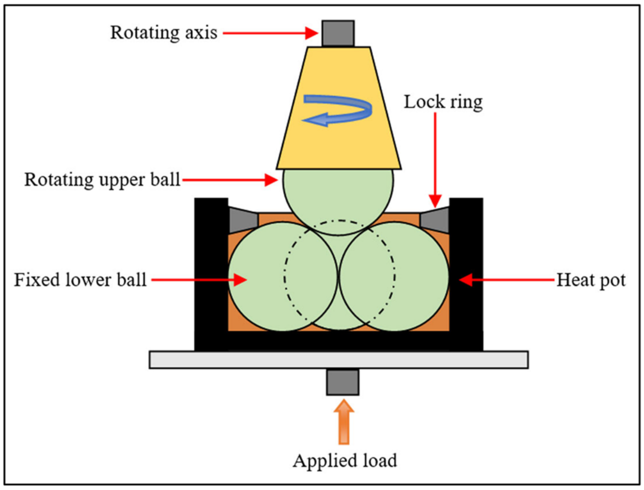

FIGURE 5 | A schematic of a four-ball tribo-tester.

from the auxiliary fuel tank scale for each running cycle. BP is calculated by Equation (1), using voltage and ampere values from the display panel and the manufacturer's provided values of power factor (ϕ) and generator efficiency (η_g) for equipment.

$$\mathrm{BP} = \frac{(V_1 I_1 + V_2 I_2 + V_3 I_3)\cos\phi}{\eta_g}, \quad (1)$$

whereas V_1, V_2, V_3 and I_1, I_2, I_3 represent the voltage and current readings, respectively. Subscripts of voltage and ampere notations indicate the repetitive testing to minimize the error.

$$\mathrm{BSFC} = \frac{\dot{m}}{\mathrm{BP}}, \quad (2)$$

$$\mathrm{BTE} = \frac{\mathrm{BP} \times 3600}{\dot{m} \times \mathrm{CV}}. \quad (3)$$

The generator efficiency varies from 80% to 85%, depending upon the electric power generated, and the power factor value is 0.85 for the experimental setup. Equations (2) and (3) were used for further calculations to obtain the data sets of engine performance evaluation for each fuel blend of known CV.

TABLE 7 | ASTM D4172 testing standard for four-ball tribo-tester.

Ball's specification	
Material of the tested balls	Carbon–chromium steel
Hardness of the tested balls	62
Diameter/size of the tested balls	12.7 mm
Roughness of ball's surface	0.04 mm
Operating factors	
Upward load under the heat pot	40 kg
Spindle rotational speed	1200 rpm
Constant temperature maintained at	75°C
Require time for each test sample	60 min

3 | Results and Discussions

3.1 | Engine Performance

Figure 6a shows the experimental results of BSFC for the diesel and six tested blends over a range of engine speeds. The overall results reveal that BSFC is higher at lower engine speeds, suggesting that engine operating conditions play a direct role in determining BSFC. Figure 6a shows that at 1100, 1200, 1300, and 1500 rpm, the B30EE10 blend and, at 1400 rpm, the B30Al blend exhibit the lowest BSFC values. It is interesting to note that at 1000 rpm, the BSFC of both blends is comparable to that of the B0 (100% diesel). Compared to diesel, B30EE15Al, B30EE10Al, and B30 show little to no improvement in terms of BSFC. When averaged over the engine speeds (see Figure 6b), the B30EE10 and B30Al blends show a 6.21% and 5.54% decrease over B0, respectively. Other fuel combinations also exhibit modest improvements in BSFC, highlighting the significance of optimizing the B30 blends with oxygenated additives (EE) and Al nanoparticles to attain the best fuel consumption efficiency. These results are consistent with the previous studies where BSFC has an overall decreasing trend with engine load and speed [28, 32, 33].

Figure 7 shows BTE for the diesel and tested blends over the tested engine speed range. In Figure 7a, the overall trend shows an increase in BTE with the increase in engine speed. Figure 7b shows that, when averaged over the engine speed, all blends show higher BTE when compared to diesel, except B30. A decrease of 4.86% in BTE is observed for B30. Other than the B30 blend, the inclusion of Al and EE has significantly improved the engine performance with increasing engine speed. B30EE10 has a higher increase in BTE, 6.02% compared to only 4.1% in B30EE15 which has a higher quantity of oxygenated additive. BTE is increased by a maximum of 6.66% for B30Al fuel blend. For EE and Al nanoparticles blend, the increase in BTE is 4.55% and 3.88% for B30EE10Al and B30EE15Al, respectively. This is consistent with previous studies given in [28, 32].

These results and their comparison with past work emphasize the need for further detailed systematic investigation to determine the best blending ratios for improving engine efficiency and reducing fuel consumption.

3.2 | Engine Emissions

Emissions are generally expected to decrease in compression ignition engines using biofuels, nanoparticles, and alcoholic additives. However, poor evaporation and atomization can lead to more CO and HC emissions as a result of improper combustion [77]. Figure 8a shows the CO concentration in the exhaust gases for all tested fuels at tested engine speeds. Figure 8b shows the CO concentrations averaged over the engine speeds.

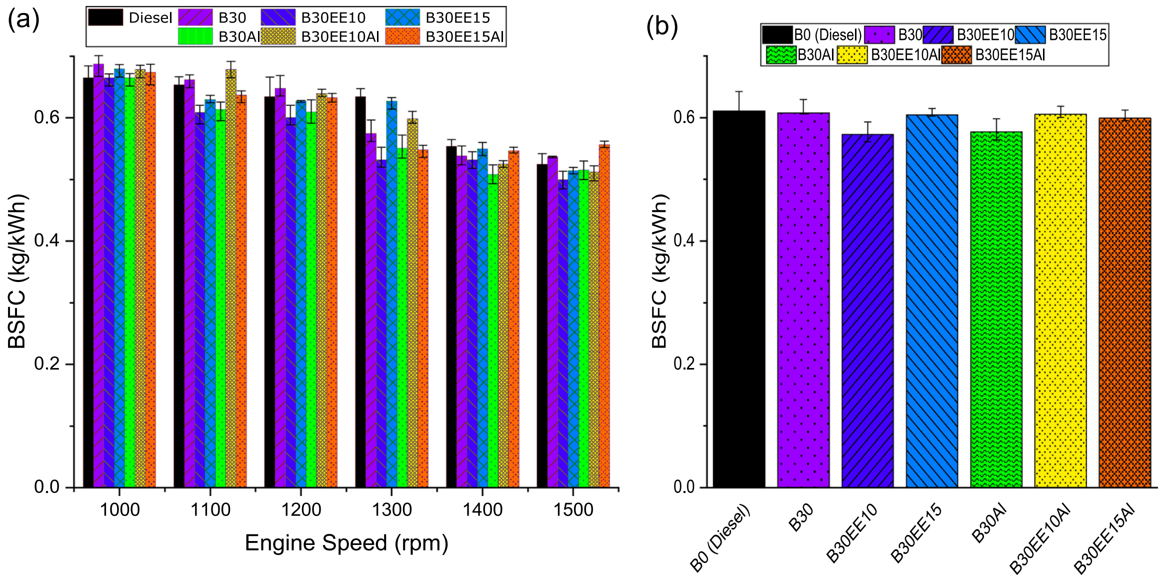

FIGURE 6 | Engine testing results of (a) brake-specific fuel consumption (BSFC) for six different speeds and (b) mean BSFC for each fuel averaged over all speeds.

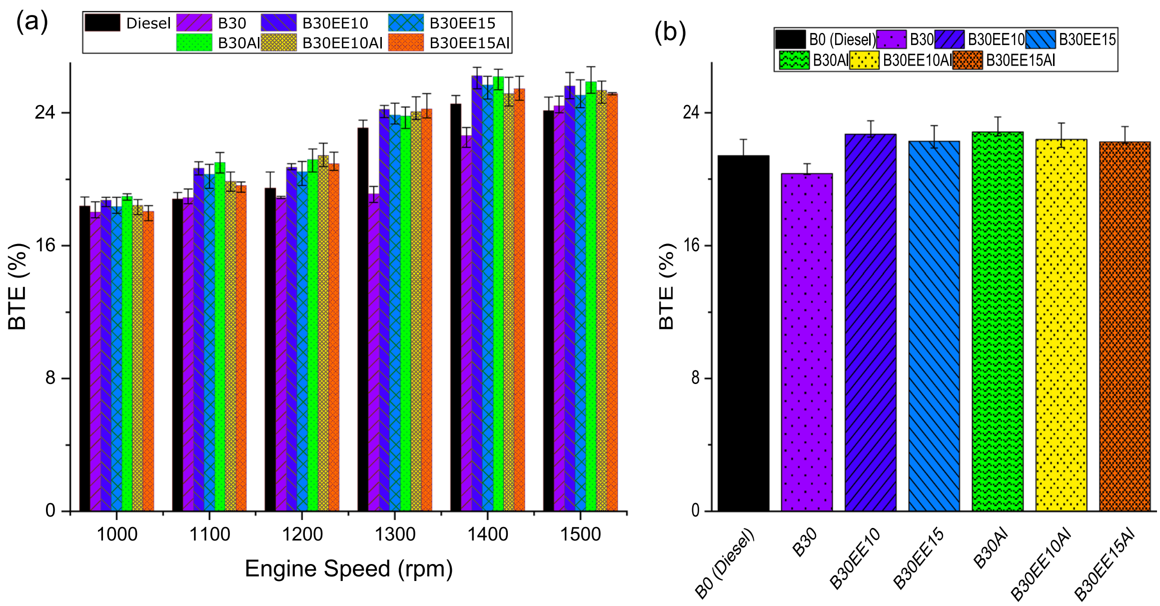

FIGURE 7 | (a) Brake thermal efficiency (BTE) of engine tests performed at various speeds and (b) mean BTE for seven different samples of fuel blends.

CO is lower at higher speeds for all blends, which is consistent with the study by Mujtaba et al. [33].

All the investigated fuel blends have shown better CO emissions than diesel. B30 and B30Al blends improve the exhaust quality, but the combination of EE and Al in blends deviates from the expected behavior. CO emissions decreased by 7.17% for B30. The blends with Al nanoparticles have shown a decrease of 18.27%, 15.27%, and 20.14% with increasing EE concentrations of 0%, 10%, and 15%, respectively. Overall, EE inclusion improves CO emissions most significantly, with B30EE10 and B30EE15 showing a reduction of 34.49% and 27.69%, respectively. This indicates that EE inclusion is effective in reducing CO emissions but up to a specific concentration. This trend is different from what was observed with Al nanoparticles, where 10% EE showed a lower decrease in CO concentration. Overall, CO emissions are least with alcoholic additives and relatively less with nanoparticles and B30 compared to diesel.

Figure 9 shows the HC emissions for increasing speed that are similar to CO emissions in Figure 8. Across the range of tested engine speeds, HC emissions show a stable downward gradient, with diesel having the highest HC production and B30 following closely after. The reduction of HC emissions in increasing order is by using B30Al, B30EE15, B30EE15Al, B30EE10Al, and B30EE10. B30EE15 and B30EE15Al showed a reduction of 26.44% and 24.55%, respectively. Interestingly, blends with 10% EE produce the least HC in exhaust gas at all engine speeds.

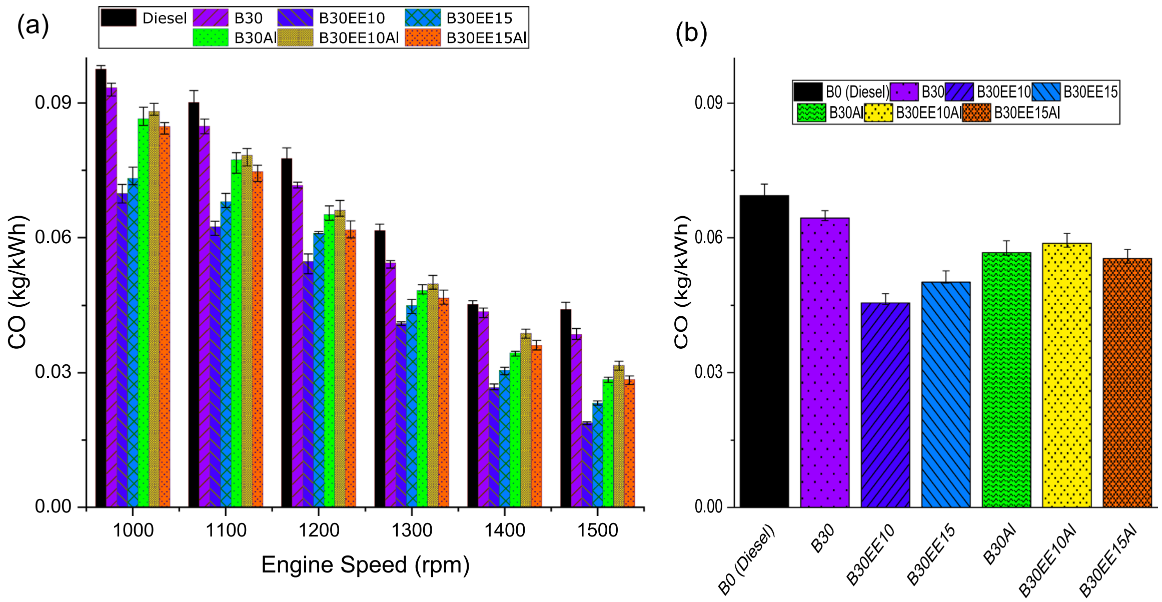

FIGURE 8 | CO emission concentration for all tested fuel samples (a) at various engine speeds. (b) Mean of CO for each fuel blend.

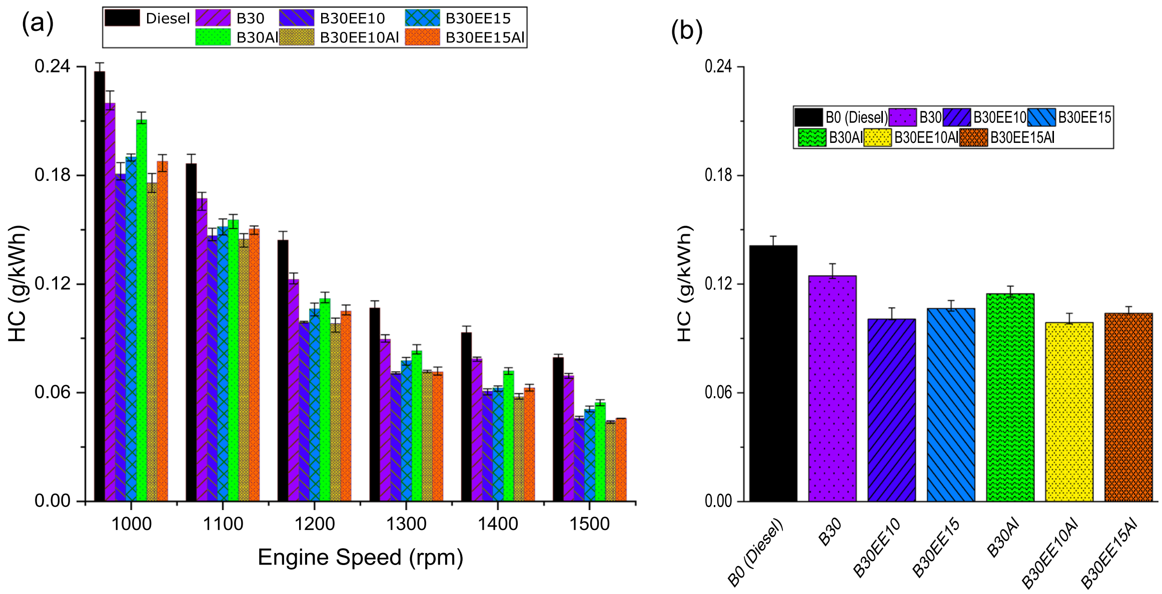

FIGURE 9 | HC emissions for various fuel samples (a) for six different speeds and (b) the mean of HC emissions.

The B30EE10Al blend exhibits the largest reduction in HC emissions, with a 30.24% decrease. Associating these results with literature gives similar trends with speed or load conditions. Commonly, HC in exhaust amounts to the lowest with the addition of oxygenated or alcoholic additives [33]; 100 ppm Al nanoparticle inclusion shows a prominent decrease in HC emissions compared to neat diesel as well as blends having lower Al nanoparticle concentrations [32].

Smog has been an alarming concern in Southeast Asia in the past few years. NO_x formation is a contributing factor to smog [7]. The use of novel biodiesels has contributed to No_x reduction in some cases while not in others. A study exploring four novel biodiesels revealed that more or less all four alternative fuels have contributed to lowering No_x compared to neat diesel [7], whereas research by the same author involving waste plastic biodiesel and Spirulina microalgae biodiesel reveals opposite results [78].

Figure 10 shows NO_x emission characteristics of the investigated fuels. Generally, the measure of NO_x emission intensity expands with increasing loads [46]. We can observe a minute general upward trend in the NO_x emissions with engine speed at a constant load of 4500 W. When averaged over the engine speeds (see Figure 10b), the blends with Al nanoparticles exhibit lower NO_x emissions compared to diesel. The lowest NO_x emission can be seen in the B30EE10Al blend, which is 3.65% less than neat diesel. B30Al and B30EE15Al blends also show a slight decrease of 1.14% and 0.95% in NO_x production, respectively. B30 showed an increase of 1.07% in NO_x emissions which increased further with EE inclusion to 3.82% and 5.98% for B30EE10 and B30EE15 respectively. In comparison with other

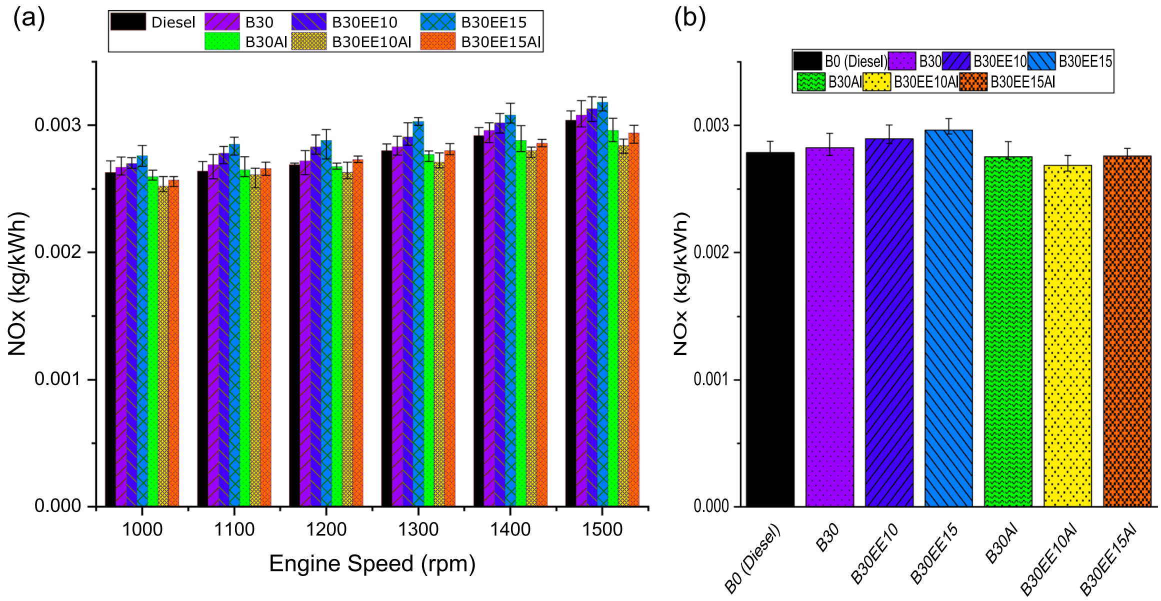

FIGURE 10 | Results for NO_x emission in combustion of litchi biodiesel and its blends (a) at various speeds and (b) mean of NO_x value for tested fuel blends.

emission parameters, NO_x values have not lowered much in this study.

EE has a lower CV than other fuels and hence lowers combustion temperatures, but its addition with other fuels is found to have a negative impact on NO_x emissions. EE's negative impact on NO_x is due to its high oxygen content. The combustion of the fuel blend improves with more oxygen, leaving a high temperature in the engine [79]. This improves the overall exhaust quality but enables the NO_x formation. The oxygenated additive EE seems to lower NO_x in diesel, but when studied with biofuel–diesel blends, it causes a negative effect on exhaust. This behavior is also backed by a study by Khalife et al. [39]. However, the reduction of NO_x is evident to some extent when EE and aluminum oxide are combined in the B30EE10Al blend.

The experimental results highlight the intricate interactions between blend compositions and how they affect diesel engine emissions. It is necessary to explore more blend compositions to get optimized results of engine performance to achieve considerable reductions in emissions without sacrificing the fuel efficiency or the engine performance. These findings support further efforts that can be made to lessen the harms of fuel combustion in engines and create sustainable transportation fuels from biomass for green energy initiatives.

3.3 | Four-Ball Tribo-Tester Frictional Analysis

Figure 11 shows the COF trend for all the tested samples mixed with SAE-40 as a base lubricant over elapsed time. The COF for diesel is above 0.11 for most of the run time, which is the highest among all tested samples. Further, the lowest COF is observed for the B30Al blend, which never reached 0.09 throughout the 60 min run time. The B30 blend showed less COF compared to diesel which improves further with an addition of EE and Al. In this section, the fuel names represent the mixture of 5% fuel mixed with 95% SAE-40 lubricating oil.

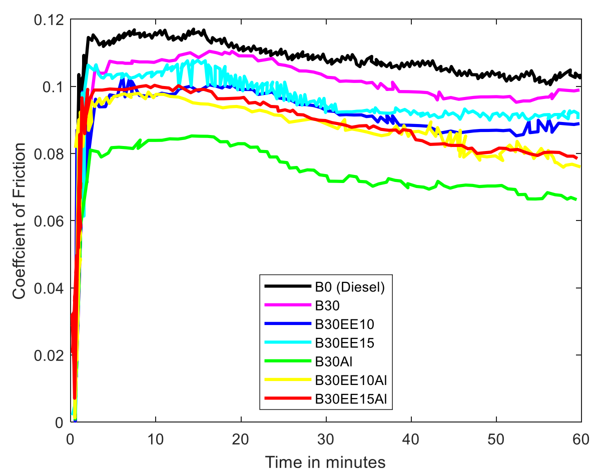

FIGURE 11 | Variation in COF versus time.

Figure 12 shows the steady-state averaged COF for blends at the time interval of 40–60 min. Here again, B30Al has the lowest COF. From Figure 12, the B30EE10 blend is observed to have a better effect on COF reduction than the B30EE15 blend. However, with the Al addition, the average COF for the B30EE15Al blend is slightly lesser than B30EE10Al, supposedly due to sudden unstable composition or low nanoparticle miscibility.

A similar pattern is observed in the studies of palm–sesame biodiesel's COF using a four-ball tribo-tester by Mujtaba et al. [34]. It is evident that the COF was lowest for base lubricant and highest for maximum diesel and decreased with the inclusion of additives, where B30 biofuel blends have a lower COF than that of diesel [34]. COF was lower for 100% biofuel (B100) compared to B30 for most of the run time except for the initiation phase of the steady state, and average COF was lower

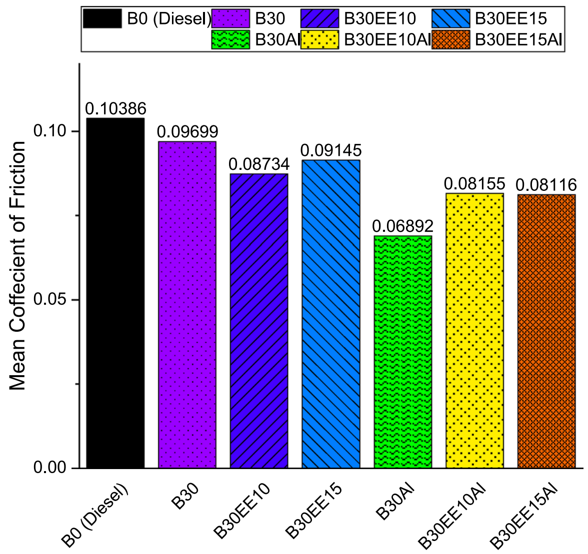

FIGURE 12 | Average COF for lubricant fuel blends at steady state.

for B100 compared to B30 and its blends with additives other than metal-oxide nanoparticle additive [80]. Overall, the best results were achieved for nanoparticle-blended mixtures, and alcoholic additives have shown variations based on their individual properties. However, their average COF values are lower than B30 and diesel fuel–lubricant blends [33].

Lower COF in any biodiesel is expected due to the presence of ester molecules that adsorb on metallic surfaces, making a film between rubbing surfaces and reducing friction, and thus preventing engine wear [81]. Moreover, *Litchi chinensis* biodiesel used in the study contains high-purity methyl esters that give it more desirable frictional properties [18]. Thus, reducing the COF of the B30 blend by 6.6% on average.

The addition of EE, with its high oxygen content, seems to reduce the COF only for low concentrations. That can be due to the low kinematic viscosity of EE, which may prevent the formation of a lubricant layer on metal surfaces [47]. The adsorption of EE on vanadium carbide (VC), which is widely used as a structural component of automobile and aircraft engines and as a grain development inhibitor in hard metals, has been shown to significantly reduce frictional properties with only minor changes in interfacial adhesion. Greater loading levels and more exposure to EE increase the friction [82, 83]. This verifies the changing behavior of increased COF for high EE content blends B3015EE and B30EE15Al compared to B30EE10 and B30EE10Alin Figure 11 which shows more EE exposure leads to more adsorption and increased COF. Figure 12, on the other hand, shows a slight decrease in COF of B30EE15Al compared to B30EE10Al.

Nanoparticles have shown decreased COF regardless of EE content, as shown in Figures 11 and 12. For a complete 60-min run time, the average COF for B30EE10Al and B30EE15Al are 6% and 9% less than B30EE10 and B30EE15 respectively. The nanoparticles-biodiesel blend B30Al shows the lowest COF among all the tested samples. Al nanoparticles act as surfactants for the fuel blends and lube oils, providing better homogeneity in all kinds of mixtures [84]. Spherical Al nanoparticles convert sliding friction between surfaces to rolling friction due to the ball-bearing effect and improved lubricating qualities by self-laminating the friction surface. As a result, in an experimental study of a four-ball test, 17.61% friction and 41.75% wear reduction were discovered for the best of 0.1% by weight of Al when testing up to 1% by weight of Al nanoparticles added to the lubricant [84]. This shows that the Al nanoparticles exhibit overall good frictional properties but only up to certain concentrations, and 100 ppm works appropriately for the 30% litchi seed biodiesel–diesel blends.

Table 8 summarizes the comparison of the present study with the findings of previous researchers' works in terms of engine performance, tailpipe emissions, and tribological parameters.

4 | Conclusion

Using a microwave-assisted transesterification method, *Litchi chinensis* biodiesel was created from LSO. The combination of 30% biodiesel and 70% diesel (B30) was mixed with EE in10% (B30EE10) and 15% (B30EE15) by volume for better oxygenation of litchi biodiesel. For further improvement of these blends, 100 ppm Al_2O_3 (abbreviated as Al) was added to create nanoparticle-infused blends (B30Al, B30EE10Al, and B30EE15Al). Sonication was performed to make homogenized nanoadditive blends for smooth engine performance and emission testing, whereas a four-ball tribo-tester was used for frictional analysis of fuel mixes. The conclusion is drawn based on the results that were obtained during the process.

- The B30EE10 blend reduced BSFC by up to 6.21%, while the B30Al blend reduced it by 5.54% while improving engine's BTE by 6.66% compared to B0.
- In terms of emissions, the B30EE10 blend achieved a 34.49% decrease in CO and a 28.72% reduction in HC emissions. The B30EE10Al blend gives optimal emissions, with an average 3.92% reduction in NO_x compared to B0.
- A four-ball tribo-tester was utilized to measure the COF of 95% SAE-40 lubricant and 5% of the fuel blends under the ASTM D4172 standard. The B30Al fuel blend has shown the lowest mean COF value of 0.068, which is 33% lower than the mean COF for B0.
- Al_2O_3 induced better frictional properties compared to oxygenated additives in the litchi seed biodiesel–diesel contaminated lube oil. However, blends with EE express intense COF variation, indicating blend instability compared to SAE-40 lubricant.

Overall, adding 100 ppm Al nanoparticles and 10% EE to 30% biodiesel (B30) made from LSO significantly improved the fuel's quality. These improvements were especially noticeable in terms of better cold flow properties (how the fuel behaves at low temperatures) and reduced emissions, making the fuel blends more efficient and environmentally friendly.

The fuel mixes containing litchi seed biodiesel, specifically the B30EE10Al blend, are recommended to be used in industries, power generation, and the transport sector as part of a pilot

TABLE 8 | Comparison of present work with other published work.

Author	Feedstock used/ method	Additives/ blends	Engine used	Results	Novelty
Mujtaba et al. [27]	50–50 palm–sesame oil/ultrasound-assisted transesterification	B30 B30 + DMC B30 + DEE B30 + CNT B30 + TiO_2	1-Cylinder, 0.638 L, CR: 17.7, radiator-cooled diesel engine	BT↑ BTE↑ HC↓ CO↓ NO_x↑	A mixture of two oils (palm–sesame) with harmonizing properties is utilized for biodiesel production and studied for the effects of alcohols and nanoparticle additives
Pullagura et al. [85]	Sea mango oil/ catalytic transesterification	SMME15 TF TF + $SiO_2$30 TF + $SiO_2$60 TF + $SiO_2$90	1-Cylinder, direct injection, liquid-cooled diesel engine	BSFC↓ BTE↑ CO↓ HC↓ NO_x↓ Smoke↓	The study investigates the effect of adding metal-based SiO_2 nanoparticles in concentrations of 30, 60, and 90 mg/L in ternary fuel (TF) mix *TF = 75% diesel + 15% sea mango methyl ester (SMME15) + 10% *iso*-butanol
Devarajan et al. [38]	Papaya seed oil/ transesterification in a 5-L batch reactor with NaOH as catalyst	Diesel BD50 BD50 + n-D BD50 + DTBP	A four-stroke, single-cylinder diesel engine	BSFC↑ BTE↓ NO_x↑ HC↓ CO↓ Smoke↓	Two oxygenated additives in a biodiesel–diesel blend are studied in diesel engine at variable brake mean effective pressure (1–5 bar) and a constant speed of 1800 rpm *n-D = decanol, DTBP = ditetrbutylperoxide
Aalam et al. [58]	Ziziphus jujube oil/ catalytic transesterification	Diesel ZJME (25%–75% biodiesel–diesel) ZJME + 25Al_2O_3 ZJME + 50Al_2O_3	A single cylinder, common-rail direct injection (CRDI) system	BTE↑ Smoke↑ SFC↑ NO_x↑ CO↓ HC↓	This study investigates the impact of a novel biodiesel, 25% blended with diesel, enhanced with 25 and 50 ppm aluminum oxide nanoparticles on combustion, performance, and emissions of a CRDI diesel engine
Present work	*Litchi chinensis* seed oil/microwave-assisted transesterification using a bio-catalyst (KOH)	B0 (diesel) B30 B30EE10 B30EE15 B30Al B30EE10Al B30EE15Al	A four-stroke, three-cylinder diesel engine	BSFC↓↑ BTE↑ HC↓ CO↓ NO_x↓↑ COF↓	Novel use of *Litchi chinensis* biodiesel mixed with oxygenated additive ethyl ethanoate (10%–15%) and Al_2O_3 nanoadditives sonicated in both biodiesel–diesel and ternary blends. The study focused on engine performance, emissions, as well as the tribological benefits of various fuel samples

project aimed at gauging the blend qualities for long-term use in engines, specifically in sectors where engine usage is inevitable. However, only with effective waste management and controlled processing of the litchiplant's seed waste can economical and green production be made possible.

The integration of diesel with biodiesel and additives for testing new biofuels promotes further research on sustainability by utilizing agricultural waste, reducing emissions, and advancing organic waste management in the transportation sector. Technological developments in nonfood biomass biodiesels have the potential to increase their sustainability and lessen competition with food supply. All things considered, biofuel research is essential to advancing clean energy, safeguarding a stable and varied energy future, and preserving the environment.

Nomenclature

Symbol	Description
EE	ethyl ethanoate/ethyl acetate
Al_2O_3	aluminum oxide
Al	100 ppm aluminum oxide nanoparticles
B30	70% diesel and 30% *Litchi chinensis* biodiesel
EE10	10% ethyl ethanoate by volume of a blend

EE15	15% ethyl ethanoate by volume of a blend
LSO	litchi seed oil
WCO	waste cooking oil
KOH	potassium hydroxide catalyst
BSFC	brake-specific fuel consumption
SFC	specific fuel consumption
BP	brake power
BTE	brake thermal efficiency
CO	carbon monoxide
HCs	hydrocarbons
NO_x	oxides of nitrogen

Acknowledgments

This research was conducted as a collaborative effort, with T.A. and T.R. contributing equally. We sincerely thank the Automotive Engineering Centre and Mechanical Engineering Department of the University of Engineering and Technology, Lahore, and the Mechanical Engineering Department of the University of Engineering and Technology, Lahore, New Campus. We also thank the College of Electrical and Mechanical Engineering of the National University of Science and Technology for their support and provision of essential equipment. We would also like to acknowledge Abu Dhabi University for partially funding this research.

References

1. *World Energy Outlook 2018* (International Energy Agency, 2018), 23–28, https://doi.org/10.1787/weo-2018-2-en.

2. R. Edwards, V. Mahieu, J.-C. Griesemann, J.-F. Larivé, and D. J. Rickeard, "Well-to-Wheels Analysis of Future Automotive Fuels and Powertrains in the European Context," 2004, https://www.jstor.org/stable/44740827.

3. *Internation Energy Agency, Monthly Oil Market Report* (IEA Press Office, 2017), www.iea.org/publications/oilmarketreport/.

4. Ü. Ağbulut and S. Sarıdemir, *A General View to Converting Fossil Fuels to Cleaner Energy Source by Adding Nanoparticles* (Taylor and Francis Ltd, 2021), https://doi.org/10.1080/01430750.2018.1563822.

5. T. M. I. Mahlia, Z. A. H. S. Syazmi, M. Mofijur, et al., "Patent Landscape Review on Biodiesel Production: Technology Updates," *Renewable and Sustainable Energy Reviews* 118 (2020): 109526, https://doi.org/10.1016/j.rser.2019.109526.

6. A. S. Rajpoot, T. Choudhary, H. M. Chelladurai, and G. Dwivedi, "A Novel Comprehensive Energy, Exergy and Sustainability Analysis of a Diesel Engine Powered by Binary Blends of Juliflora Biodiesel and Nanoparticles," *Journal of Thermal Analysis and Calorimetry* 148, no. 21 (2023): 11981–11997, https://doi.org/10.1007/s10973-023-12473-x.

7. A. S. Rajpoot, T. Choudhary, H. M. Chelladurai, A. A. Sinha, and H. Pachori, "Comparative Thermal Assessment and Emission Analysis of Various Green Biodiesel From Novel Feedstocks for CI Engines: A Sustainable Approach Towards Emission Reduction," *Environmental Science and Pollution Research* 31, no. 27 (2024): 39650–39662, https://doi.org/10.1007/s11356-024-33817-6.

8. J. Tomei and R. Helliwell, "Food Versus Fuel? Going Beyond Biofuels," 2016, http://www.eoi.es/blogs/julianamejia/2013/02/12/biofuels-vs-food-security/.

9. M. Abdul Hakim Shaah, M. S. Hossain, F. A. Salem Allafi, et al., "A Review on Non-Edible Oil as a Potential Feedstock for Biodiesel: Physicochemical Properties and Production Technologies," *RSC Advances* 11, no. 40 (2021): 25018–25037, https://doi.org/10.1039/d1ra04311k.

10. A. E. Atabani, S. Shobana, M. N. Mohammed, et al., "Integrated Valorization of Waste Cooking Oil and Spent Coffee Grounds for Biodiesel Production: Blending With Higher Alcohols, FT-IR, TGA, DSC and NMR Characterizations," *Fuel* 244 (2019): 419–430, https://doi.org/10.1016/j.fuel.2019.01.169.

11. P. S. Nigam and A. Singh, "Production of Liquid Biofuels From Renewable Resources," *Progress in Energy and Combustion Science* 37 (2011): 52–68, https://doi.org/10.1016/j.pecs.2010.01.003.

12. E. S. Shuba and D. Kifle, "Microalgae to Biofuels: 'Promising' Alternative and Renewable Energy, Review," *Renewable and Sustainable Energy Reviews* 81 (2018): 743–755, https://doi.org/10.1016/j.rser.2017.08.042.

13. I. Kralova and J. Sjöblom, "Biofuels-Renewable Energy Sources: A Review," *Journal of Dispersion Science and Technology* 31, no. 3 (Mar 2010): 409–425, https://doi.org/10.1080/01932690903119674.

14. S. Emanuele, M. Lauricella, G. Calvaruso, A. D'Anneo, and M. Giuliano, "*Litchi chinensis* as a Functional Food and a Source of Antitumor Compounds: An Overview and a Description of Biochemical Pathways," *Nutrients* 9 (2017): 992, https://doi.org/10.3390/nu9090992.

15. S. P. Bangar, M. Kumar, W. S. Whiteside, M. Tomar, and J. F. Kennedy, "Litchi (*Litchi chinensis*) Seed Starch: Structure, Properties, and Applications—A Review," *Carbohydrate Polymer Technologies and Applications* 2 (2021): 100080, https://doi.org/10.1016/j.carpta.2021.100080.

16. Y. Singh, D. Singh, N. K. Singh, et al., "Production of Bio-Oil From Lychee-Based Biomass Through Pyrolysis and Maximization of Bio-Oil Yield With Statistical and Machine Learning Techniques," *Journal of Cleaner Production* 413 (Aug 2023): 137472, https://doi.org/10.1016/j.jclepro.2023.137472.

17. P. Verma, M. P. Sharma, and G. Dwivedi, "Evaluation and Enhancement of Cold Flow Properties of Palm Oil and Its Biodiesel," *Energy Reports* 2 (2016): 8–13, https://doi.org/10.1016/j.egyr.2015.12.001.

18. T. Asif, F. Noor, S. Imran, et al., "Microwave-Assisted Transesterification of *Litchi chinensis* Seed Oil Using Extracted KOH From Potato Waste for Sustainable Development," *Frontiers in Energy Research* 11 (Jan 2024): 1339601, https://doi.org/10.3389/fenrg.2023.1339601.

19. A. E. Atabani, T. M. I. Mahlia, I. Anjum Badruddin, H. H. Masjuki, W. T. Chong, and K. T. Lee, "Investigation of Physical and Chemical Properties of Potential Edible and Non-Edible Feedstocks for Biodiesel Production, a Comparative Analysis," *Renewable and Sustainable Energy Reviews* 21 (2013): 749–755, https://doi.org/10.1016/j.rser.2013.01.027.

20. M. Gul, H. H. Masjuki, M. A. Kalam, N. W. M. Zulkifli, and M. A. Mujtaba, "A Review: Role of Fatty Acids Composition in Characterizing Potential Feedstock for Sustainable Green Lubricants by Advance Transesterification Process and Its Global as Well as Pakistani Prospective," *BioEnergy Research* 12 (2020): 1–22, https://doi.org/10.1007/s12155-019-10040-7.

21. I. M. Monirul, H. H. Masjuki, M. A. Kalam, et al., "A Comprehensive Review on Biodiesel Cold Flow Properties and Oxidation Stability Along With Their Improvement Processes," *RSC Advances* 5, no. 105 (2015): 86631–86655, https://doi.org/10.1039/c5ra09555g.

22. R. Dhairiyasamy, W. Bunpheng, C. C. Kit, and N. Hasan, "Comparative Performance and Emission Analysis of Soybean and Algae Biodiesels in Low Heat Rejection Engines," *Energy Science & Engineering* 13 (2025): 1732–1748, https://doi.org/10.1002/ese3.2090.

23. P. M. Ndiaye, E. Franceschi, D. Oliveira, C. Dariva, F. W. Tavares, and J. V. Oliveira, "Phase Behavior of Soybean Oil, Castor Oil and Their Fatty Acid Ethyl Esters in Carbon Dioxide at High Pressures," *Journal of Supercritical Fluids* 37, no. 1 (2006): 29–37, https://doi.org/10.1016/j.supflu.2005.08.002.

24. P. A. Leggieri, M. Senra, and L. Soh, "Cloud Point and Crystallization in Fatty Acid Ethyl Ester Biodiesel Mixtures With and Without Additives," *Fuel* 222 (2018): 243–249, Jun., https://doi.org/10.1016/j.fuel.2018.02.100.

25. A. H. Kadarohman, F. Khoerunisa, and R. M. Astuti, "A Potential Study on Clove Oil, Eugenol and Eugenyl Acetate as Diesel Fuel Bio-Additives and Their Performance on One Cylinder Engine," *Transport* 25, no. 1 (2010): 66–76, https://doi.org/10.3846/transport.2010.09.

26. M. E. M. Soudagar, N. N. Nik-Ghazali, M. Abul Kalam, I. A. Badruddin, N. R. Banapurmath, and N. Akram, "The Effect of Nano-Additives in Diesel–Biodiesel Fuel Blends: A Comprehensive Review on Stability, Engine Performance and Emission Characteristics," *Energy Conversion and Management* 178 (2018): 146–177, https://doi.org/10.1016/j.enconman.2018.10.019.

27. M. A. Mujtaba, M. A. Kalam, H. H. Masjuki, et al., "Comparative Study of Nanoparticles and Alcoholic Fuel Additives-Biodiesel–Diesel Blend for Performance and Emission Improvements," *Fuel* 279 (Nov 2020): 118434, https://doi.org/10.1016/j.fuel.2020.118434.

28. Ü. Ağbulut, M. Karagöz, S. Sarıdemir, and A. Öztürk, "Impact of Various Metal-Oxide Based Nanoparticles and Biodiesel Blends on the Combustion, Performance, Emission, Vibration and Noise Characteristics of a CI Engine," *Fuel* 270 (Jun 2020): 117521, https://doi.org/10.1016/j.fuel.2020.117521.

29. A. Çakmak, *Improvement of Exhaust Emissions in a Diesel Engine With the Addition of an Oxygenated Additive to Diesel–Biodiesel Blends* (2022).

30. S. K. Musyoka, A. S. G. Khalil, S. A. Ookawara, and A. E. Elwardany, "Effect of C4 Alcohol and Ester as Fuel Additives on Diesel Engine Operating Characteristics," *Fuel* 341 (Jun 2023): 127656, https://doi.org/10.1016/j.fuel.2023.127656.

31. M. E. M. Soudagar, N. N. Nik-Ghazali, M. A. Kalam, et al., "An Investigation on the Influence of Aluminium Oxide Nano-Additive and Honge Oil Methyl Ester on Engine Performance, Combustion and Emission Characteristics," *Renewable Energy* 146 (Feb 2020): 2291–2307, https://doi.org/10.1016/j.renene.2019.08.025.

32. M. A. Fayad and H. A. Dhahad, "Effects of Adding Aluminum Oxide Nanoparticles to Butanol–Diesel Blends on Performance, Particulate Matter, and Emission Characteristics of Diesel Engine," *Fuel* 286 (Feb 2021): 119363, https://doi.org/10.1016/j.fuel.2020.119363.

33. M. A. Mujtaba, H. H. Masjuki, M. A. Kalam, et al., "Effect of Additivized Biodiesel Blends on Diesel Engine Performance, Emission, Tribological Characteristics, and Lubricant Tribology," *Energies* 13, no. 13 (Jul 2020): 3375, https://doi.org/10.3390/en13133375.

34. M. A. Mujtaba, M. A. Kalam, H. H. Masjuki, et al., "Effect of Palm–Sesame Biodiesel Fuels With Alcoholic and Nanoparticle Additives on Tribological Characteristics of Lubricating Oil by Four Ball Tribo-Tester," *Alexandria Engineering Journal* 60, no. 5 (Oct 2021): 4537–4546, https://doi.org/10.1016/j.aej.2021.03.017.

35. S. Imtenan, H. H. Masjuki, M. Varman, et al., "Impact of Oxygenated Additives to Palm and Jatropha Biodiesel Blends in the Context of Performance and Emissions Characteristics of a Light-Duty Diesel Engine," *Energy Conversion and Management* 83 (2014): 149–158, https://doi.org/10.1016/j.enconman.2014.03.052.

36. A. S. Rajpoot, T. Choudhary, H. M. Chelladurai, U. Rajak, and A. A. Sinha, "Effect of Oxyhydrogen as on Energy, Exergy and Sustainability Analysis of a Diesel Engine Fueled With Palm Oil Biodiesel," *Proceedings of the Institution of Mechanical Engineers, Part E: Journal of Process Mechanical Engineering* (2024): 09544089241259758, https://doi.org/10.1177/09544089241259758.

37. R. Jayabal, L. Thangavelu, and S. Subramani, "Combined Effect of Oxygenated Additives, Injection Timing and EGR on Combustion, Performance and Emission Characteristics of a CRDi Diesel Engine Powered by Sapota Biodiesel/Diesel Blends," *Fuel* 276 (Sep 2020): 118020, https://doi.org/10.1016/j.fuel.2020.118020.

38. Y. Devarajan, N. Beemkumar, S. Ganesan, and T. Arunkumar, "An Experimental Study on the Influence of an Oxygenated Additive in Diesel Engine Fuelled With Neat Papaya Seed Biodiesel/Diesel Blends," *Fuel* 268 (May 2020): 117254, https://doi.org/10.1016/j.fuel.2020.117254.

39. E. Khalife, M. Tabatabaei, A. Demirbas, and M. Aghbashlo, "Impacts of Additives on Performance and Emission Characteristics of Diesel Engines During Steady State Operation," *Progress in Energy and Combustion Science* 59 (2017): 32–78, https://doi.org/10.1016/j.pecs.2016.10.001.

40. L. Xu, Y. Wang, and D. Liu, "Effects of Oxygenated Biofuel Additives on Soot Formation: A Comprehensive Review of Laboratory-Scale Studies," *Fuel* 313 (2022): 122635, https://doi.org/10.1016/j.fuel.2021.122635.

41. M. A. Mujtaba, H. Muk Cho, H. H. Masjuki, et al., "Effect of Primary and Secondary Alcohols as Oxygenated Additives on the Performance and Emission Characteristics of Diesel Engine," *Energy Reports* 7 (Nov 2021): 1116–1124, https://doi.org/10.1016/j.egyr.2020.12.008.

42. J. R. Bikkavolu, S. Vadapalli, K. R. R. Chebattina, and G. Pullagura, "Investigation of the Effect of Adding Carbon Nanotubes, Lower and Higher Level Alcohol Additives, in Yellow Oleander Methyl Ester-Diesel Blend on Diesel Engine Performance," *Energy Sources, Part A: Recovery, Utilization, and Environmental Effects* 45, no. 4 (2023): 11619–11636, https://doi.org/10.1080/15567036.2023.2263416.

43. S. Ahmad, A. T. Jafry, M. ul Haq, et al., "Performance and Emission Characteristics of Second-Generation Biodiesel With Oxygenated Additives," *Energies* 16 (2023): 5153, https://doi.org/10.3390/en16135153.

44. V. D. Raju, H. Venu, L. Subramani, P. S. Kishore, P. L. Prasanna, and D. V. Kumar, "An Experimental Assessment of Prospective Oxygenated Additives on the Diverse Characteristics of Diesel Engine Powered With Waste Tamarind Biodiesel," *Energy* 203 (Jul 2020): 117821, https://doi.org/10.1016/j.energy.2020.117821.

45. B. Deepanraj, P. Lawrence, M. Kannan, V. Nadanakumar, S. Santhanakrishnan, and R. Senthil, "Study on Performance and Emission Characteristics of a Compression Ignition Engine Fueled With Diesel-2 Ethoxy Ethyl Acetate Blends," *Engineering* 03, no. 11 (2011): 1132–1136, https://doi.org/10.4236/eng.2011.311141.

46. A. I. El-Seesy, M. Nour, H. Hassan, A. Elfasakhany, Z. He, and M. A. Mujtaba, "Diesel-Oxygenated Fuels Ternary Blends With Nano Additives in Compression Ignition Engine: A Step Towards Cleaner Combustion and Green Environment," *Case Studies in Thermal Engineering* 25 (Jun 2021): 100911, https://doi.org/10.1016/j.csite.2021.100911.

47. L. Aguado-Deblas, R. Estevez, J. Hidalgo-Carrillo, et al., "Outlook for Direct Use of Sunflower and Castor Oils as Biofuels in Compression Ignition Diesel Engines, Being Part of Diesel/Ethyl Acetate/Straight Vegetable Oil Triple Blends," *Energies* 13, no. 18 (Sep 2020): 4836, https://doi.org/10.3390/en13184836.

48. M. Gul, A. N. Shah, U. Aziz, et al., "Grey-Taguchi and ANN Based Optimization of a Better Performing Low-Emission Diesel Engine Fueled With Biodiesel," *Energy Sources, Part A: Recovery, Utilization, and Environmental Effects.* 44, no. 1 (2022): 1019–1032, https://doi.org/10.1080/15567036.2019.1638995.

49. S. S. P. Sundar, P. Vijayabalan, R. Sathyamurthy, A. E. Kabeel, and K. Kamalakkannan, "An Experimental Approach on the Utilization of Palm Oil Biodiesel With Higher Concentration of Al_2O_3 Nanoadditive for Performance Enhancement and Emission Reduction," *Environmental Science and Pollution Research* 29, no. 59 (Dec 2022): 89411–89425, https://doi.org/10.1007/s11356-022-22028-6.

50. K. Nanthagopal, B. Ashok, A. Tamilarasu, A. Johny, and A. Mohan, "Influence on the Effect of Zinc Oxide and Titanium Dioxide Nanoparticles as an Additive With *Calophyllum inophyllum* Methyl Ester in a CI Engine," *Energy Conversion and Management* 146 (2017): 8–19, https://doi.org/10.1016/j.enconman.2017.05.021.

51. M. Valihesari, V. Pirouzfar, F. Ommi, and F. Zamankhan, "Investigating the Effect of Fe_2O_3 and TiO_2 Nanoparticle and Engine Variables on the Gasoline Engine Performance Through Statistical Analysis," *Fuel* 254 (Oct 2019): 115618, https://doi.org/10.1016/j.fuel.2019.115618.

52. Z. Zhang, Y. Lu, Y. Wang, et al., "Comparative Study of Using Multi-Wall Carbon Nanotube and Two Different Sizes of Cerium Oxide Nanopowders as Fuel Additives under Various Diesel Engine Conditions," *Fuel* 256 (Nov 2019): 115904, https://doi.org/10.1016/j.fuel.2019.115904.

53. R. Sabarish, S. Jenoris Muthiya, B. Anandan, et al., "The Role and Impact of Al_2O_3 Additive on the Performance of the Diesel Engine Operated by JFO Along With Its Measures of Combustion and Emissions," *Energy Science & Engineering* 13 (2025): 995–1010, https://doi.org/10.1002/ese3.2064.

54. M. E. M. Soudagar, N.-N. Nik-Ghazali, M. A. Kalam, et al., "The Effects of Graphene Oxide Nanoparticle Additive Stably Dispersed in Dairy Scum Oil Biodiesel–Diesel Fuel Blend on CI Engine: Performance, Emission and Combustion Characteristics," *Fuel* 257 (Dec 2019): 116015, https://doi.org/10.1016/j.fuel.2019.116015.

55. Y. Kaushik, V. Verma, K. K. Saxena, C. Prakash, L. R. Gupta, and S. Dixit, "Effect of Al_2O_3 Nanoparticles on Performance and Emission Characteristics of Diesel Engine Fuelled With Diesel–Neem Biodiesel Blends," *Sustain* 14, no. 13 (Jul 2022): 7913, https://doi.org/10.3390/su14137913.

56. A. Backiyaraj, M. Parthasarathy, N. Murugu Nachippan, P. B. Senthilkumar, and T. Kumaran, "Influence of Nano Al_2O_3 on Compression Ignition Engine Characteristics Fuelled With Mahua Biodiesel," *Materials Today: Proceedings* 72 (Jan 2023): 2238–2244, https://doi.org/10.1016/j.matpr.2022.09.210.

57. A. Z. Hameed and K. Muralidharan, "Performance, Emission, and Catalytic Activity Analysis of Al_2O_3 and CeO_2 Nano-Additives on Diesel Engines Using Mahua Biofuel for a Sustainable Environment," *ACS Omega* 8, no. 6 (2023): 5692–5701, Feb., https://doi.org/10.1021/acsomega.2c07193.

58. C. S. Aalam, C. G. Saravanan, and M. Kannan, "Experimental Investigations on a CRDI System Assisted Diesel Engine Fuelled With Aluminium Oxide Nanoparticles Blended Biodiesel," *Alexandria Engineering Journal* 54, no. 3 (Mar 2015): 351–358, https://doi.org/10.1016/j.aej.2015.04.009.

59. R. Niculescu, A. Clenci, and V. Iorga-Siman, "Review on the Use of Diesel–Biodiesel–Alcohol Blends in Compression Ignition Engines," *Energies* 12, no. 7 (2019): 1194, https://doi.org/10.3390/en12071194.

60. M. S. Gad, Ü. Ağbulut, A. Afzal, et al., "A Comprehensive Review on the Usage of the Nano-Sized Particles Along With Diesel/Biofuel Blends and Their Impacts on Engine Behaviors," *Fuel* 339 (2023): 127364, https://doi.org/10.1016/j.fuel.2022.127364.

61. A. Ruggiero, R. D'Amato, R. Calvo, P. Valašek, and N. Ungureanu, "Measurements of the Friction Coefficient: Discussion on the Results in the Framework of the Time Series Analysis," in *Advances in Manufacturing Engineering and Materials: Lecture Notes in Mechanical Engineering*, ed. S. Hloch, D. Klichová, G. Krolczyk, S. Chattopadhyaya, L. Ruppenthalová (Springer, 2019), 443–455, https://doi.org/10.1007/978-3-319-99353-9_47.

62. H. H. Masjuki, M. A. Kalam, M. Syazly, et al., "Experimental Evaluation of an Unmodified Diesel Engine Using Biodiesel With Fuel Additive," in *International Forum on Strategic Technology* (2006).

63. D. Kumar, A. Kumar, A. Singla, and R. Dewan, "Production and Tribological Characterization of Castor Based Biodiesel," *Materials Today: Proceedings* 46 (2021): 10942–10949, https://doi.org/10.1016/j.matpr.2021.02.009.

64. V. Goel, N. Kumar, P. Singh, M. A. Fazal, and M. M. Quazi, "Tribological Analysis of Novel *Jasminum officinale* Biodiesel Blends by Using Four-Ball Tribotester," *Journal of the Brazilian Society of Mechanical Sciences and Engineering* 44 (Nov 2022): 497, https://doi.org/10.1007/s40430-022-03795-2.

65. C.-M. Lai, D. L. Loo, Y. H. Teoh, et al., "Optimization and Performance Characteristics of Diesel Engine Using Green Fuel Blends With Nanoparticles Additives," *Fuel* 347 (Sep 2023): 128462, https://doi.org/10.1016/j.fuel.2023.128462.

66. B. Suresha, G. Hemanth, A. Rakesh, and K. M. Adarsh, "Tribological Behaviour of Neem Oil With and Without Graphene Nanoplatelets Using Four-Ball Tester," *Advances in Tribology* 2020 (2020): 1984931, https://doi.org/10.1155/2020/1984931.

67. S. Ghalme, P. Koinkar, Y. Bhalerao, and S. G. Ghalme, "Tribology in Industry Effect of Aluminium Oxide (Al_2O_3) Nanoparticles Addition Into Lubricating Oil on Tribological Performance," www.tribology.rs.

68. D. L. Loo, Y. H. Teoh, H. G. How, et al., "Effect of Nanoparticles Additives on Tribological Behaviour of Advanced Biofuels," *Fuel* 334 (Feb 2023): 126798, https://doi.org/10.1016/j.fuel.2022.126798.

69. J. Milano, H. C. Ong, H. H. Masjuki, et al., "Optimization of Biodiesel Production by Microwave Irradiation-Assisted Transesterification for Waste Cooking Oil-*Calophyllum inophyllum* Oil via Response Surface Methodology," *Energy Conversion and Management* 158 (Feb 2018): 400–415, https://doi.org/10.1016/j.enconman.2017.12.027.

70. M. A. Mujtaba, H. H. Masjuki, M. A. Kalam, et al., "Ultrasound-Assisted Process Optimization and Tribological Characteristics of Biodiesel From Palm–Sesame Oil via Response Surface Methodology and Extreme Learning Machine - Cuckoo Search," *Renewable Energy* 158 (Oct 2020): 202–214, https://doi.org/10.1016/j.renene.2020.05.158.

71. "Standard Specification for Biodiesel Fuel Blend Stock (B100), ASTM D6751-23," ASTM International, 2023.

72. "Liquid Petroleum Products—Fatty Acid Methyl Esters (FAME) for Use in Diesel Engines and Heating Applications—Requirements and Test Methods, EN 14214," European Committee for Standardization, 2019.

73. "Aluminum Oxide (Al_2O_3) Nanopowder," Nanostructured & Amorphous Materials Inc., 2017, https://www.nanoamor.com/inc/sdetail/23066.

74. S. Gumus, H. Ozcan, M. Ozbey, and B. Topaloglu, "Aluminum Oxide and Copper Oxide Nanodiesel Fuel Properties and Usage in a Compression Ignition Engine," *Fuel* 163 (Jan 2016): 80–87, https://doi.org/10.1016/j.fuel.2015.09.048.

75. A. Qamar, Z. Anwar, H. Ali, et al., "Preparation and Dispersion Stability of Aqueous Metal Oxide Nanofluids for Potential Heat Transfer Applications: A Review of Experimental Studies," *Journal of Thermal Analysis and Calorimetry* 147, no. 1 (2022): 23–46, https://doi.org/10.1007/s10973-020-10372-z.

76. V. Saxena, N. Kumar, and V. K. Saxena, "A Comprehensive Review on Combustion and Stability Aspects of Metal Nanoparticles and Its Additive Effect on Diesel and Biodiesel Fuelled C.I. Engine," *Renewable and Sustainable Energy Reviews* 70, no. September 2016 (2017): 563–588, https://doi.org/10.1016/j.rser.2016.11.067.

77. J. R. Bikkavolu, G. Pullagura, V. V. S. Prasad, et al., "Employing Hydrogen Infusion to Improve the Combustion Attributes of Di-Methyl Carbonate-Boron Nitride-Biodiesel/Diesel Blends in a Diesel Engine," *International Journal of Hydrogen Energy* 143 (2025): 389–402, https://doi.org/10.1016/j.ijhydene.2024.12.447.

78. A. S. Rajpoot, T. Choudhary, A. K. Chauhan, H. Pachori, and M. Sharma, "Thermal and Emission Analysis of Waste Plastic and Microalgae Biodiesel as a Potential Power Source for Diesel Engines: A Sustainable Approach," *Environmental Science and Pollution Research* 31, no. 50 (2024): 59961–59976, https://doi.org/10.1007/s11356-024-35137-1.

79. M. Santasnachok, E. Sutheerasak, C. Chinwanitcharoen, W. Ruengphrathuengsuka, and S. Chuepeng, "Use of Diesel Mixed With Ethanol and Ethyl Acetate for Alternative Fuel in a High-Speed Diesel Engine," 2021.

80. M. A. Mujtaba, H. Muk Cho, H. H. Masjuki, et al., "Effect of Alcoholic and Nano-Particles Additives on Tribological Properties of Diesel–Palm–Sesame–Biodiesel Blends," *Energy Reports* 7 (Nov 2021): 1162–1171, https://doi.org/10.1016/j.egyr.2020.12.009.

81. J. Milano, A. H. Shamsuddin, A. S. Silitonga, et al., "Tribological Study on the Biodiesel Produced From Waste Cooking Oil, Waste Cooking Oil Blend With *Calophyllum inophyllum* and Its Diesel Blends on Lubricant Oil," *Energy Reports* 8 (Nov 2022): 1578–1590, https://doi.org/10.1016/j.egyr.2021.12.059.

82. A. S. Kurlov, A. I. Gusev, E. Y. Gerasimov, I. A. Bobrikov, A. M. Balagurov, and A. A. Rempel, "Nanocrystalline Ordered Vanadium Carbide: Superlattice and Nanostructure," *Superlattices and Microstructures* 90 (Feb 2016): 148–164, https://doi.org/10.1016/j.spmi.2015.12.006.

83. L. C. Fernández-Torres, X. Zhao, Z. Chen, C. Salmeron, and S. S. Perry, "Influence of Ethyl Acetate and Alkyl Phosphate Adsorption on the Frictional Properties of VC(100)," *Tribology Letters* 18, no. 2 (Feb 2005): 207–213, https://doi.org/10.1007/s11249-004-1777-4.

84. T. Luo, X. Wei, X. Huang, L. Huang, and F. Yang, "Tribological Properties of Al_2O_3 Nanoparticles as Lubricating Oil Additives," *Ceramics International* 40, no. 5 (Jun 2014): 7143–7149, https://doi.org/10.1016/j.ceramint.2013.12.050.

85. G. Pullagura, J. R. Bikkavolu, S. Vadapalli, et al., "Performance, Combustion and Emission Reduction Characteristics of Metal-Based Silicon Dioxide Nanoparticle Additives Included in Ternary Fuel (Diesel–SMME–*Iso* Butanol) on Diesel Engine," *Heliyon* 10, no. 4 (2024): e26519, https://doi.org/10.1016/j.heliyon.2024.e26519.